

## Supporting Information

### Polyaniline-grafted Hydrolysed Polyethylene as a Dual Functional Interlayer/Separator for High-Performance Li-S@C Core-Shell Batteries

Suchakree Tubtimkuna<sup>a,b</sup>, Atiweena Krittayavathananon<sup>a,b</sup>, Poramane Chiochan<sup>a,b</sup>, Salatan Duangdangchote<sup>a,b</sup>, Juthaporn Wutthiprom<sup>a,b</sup>, Jumras Limtrakul<sup>a,b</sup> and Montree Sawangphruk<sup>a,b</sup>

<sup>a</sup>Department of Chemical and Biomolecular Engineering, School of Energy Science and Engineering, Vidyasirimedhi Institute of Science and Technology, Rayong 21210, Thailand

<sup>b</sup>Centre of Excellence for Energy Storage Technology (CEST), Vidyasirimedhi Institute of Science and Technology, Rayong 21210, Thailand

## Experimental

### *Chemicals and materials*

Potassium permanganate (KMnO<sub>4</sub>, Carlo Erba), sulfuric acid (H<sub>2</sub>SO<sub>4</sub>, 98%, QRëC), aniline monomer (C<sub>6</sub>H<sub>5</sub>NH<sub>2</sub>, Appli chem Panreac), hydrochloric acid (HCl, 37%, QRëC), ammonium persulfate ((NH<sub>4</sub>)<sub>2</sub>S<sub>2</sub>O<sub>8</sub>, LOBA chemie), N-(3-Dimethylaminopropyl)-N'-ethylcarbodiimide hydrochloride (C<sub>8</sub>H<sub>17</sub>N<sub>3</sub> · HCl, Sigma-Aldrich), N-hydroxysuccinimide (C<sub>4</sub>H<sub>5</sub>NO<sub>3</sub>, Sigma-Aldrich), N-methyl-2-pyrrolidone (NMP, QRëC), anhydrous lithium nitrate (LiNO<sub>3</sub>, Alfa Aesar), lithium bis(trifluoromethane)sulfonimide (LiTFSI, Sigma-Aldrich), 1,3-dioxolane (DOL, Alfa Aesar), anhydrous 1,2-dimethoxyethane (DME, Sigma-Aldrich), and polyvinylidene fluoride (PVDF, Mw=534000 g mol<sup>-1</sup>, Sigma-Aldrich) were of analytical grade and used without further purification. Polyethylene (PE, a thickness of 0.030 mm) and hydrolyse polyethylene (HyPE, a thickness of 0.161 mm) separators were obtained from Gelon LIB Co., Ltd, Hong Kong. Carbon fibre paper (0.264 mm thickness, GDL 39 BA) was purchased from SGL CARBON SE, Germany and used as a substrate. Deionized water was purified by using a Milli-Q system (DI water, 15 MΩ.cm, Millipore).

### *Modification of hydrolysed polyethylene by grafting with polyaniline (HyPE-PANI)*

Firstly, HyPE (8 × 7 cm<sup>2</sup>) with a thickness of ca. 160 μm (Celgard) was modified to have carboxyl functional groups (-COOH) on its surface by immersing it in a 400-mL strong oxidizing agent (2 g L<sup>-1</sup> KMnO<sub>4</sub> in H<sub>2</sub>SO<sub>4</sub>) for ca. 10 min at room temperature, washed with DI water many times and dried overnight at 60°C<sup>1</sup> (see Fig. S1).

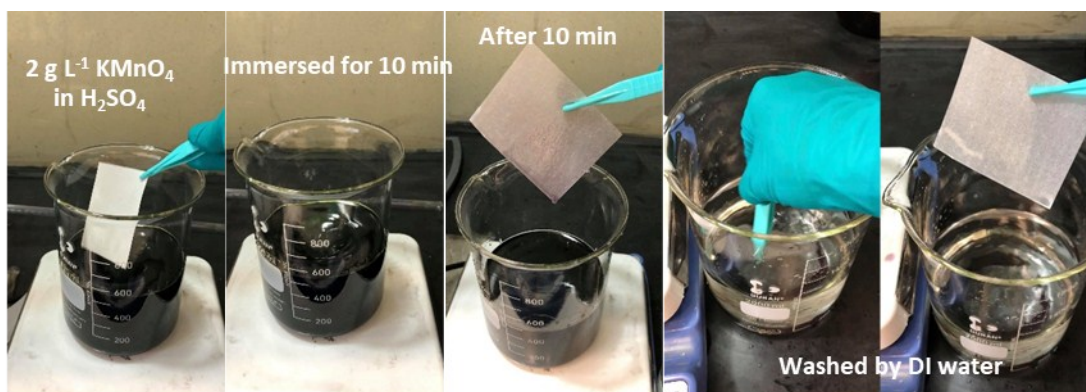


Fig. S1 Surface modification of HyPE with carboxyl functional groups.

After that, 8.33 mL of aniline monomer was added into the mixture of DI water (500 mL) and HCl (50 mL). The solution was stirred for 15 min in an ice bath controlling the temperature to maintain at 0-5 °C. 0.25 M ammonium persulfate solution (18.924 g  $(\text{NH}_4)_2\text{S}_2\text{O}_8$  dissolved in 330 mL DI water) was added dropwise to a cooled mixture while kept stirring for 24 h. Note, HCl and  $(\text{NH}_4)_2\text{S}_2\text{O}_8$  act as the oxidant and initiator, respectively. The pH of as-obtained PANI was adjusted until neutral with DI water (see Fig. S2).

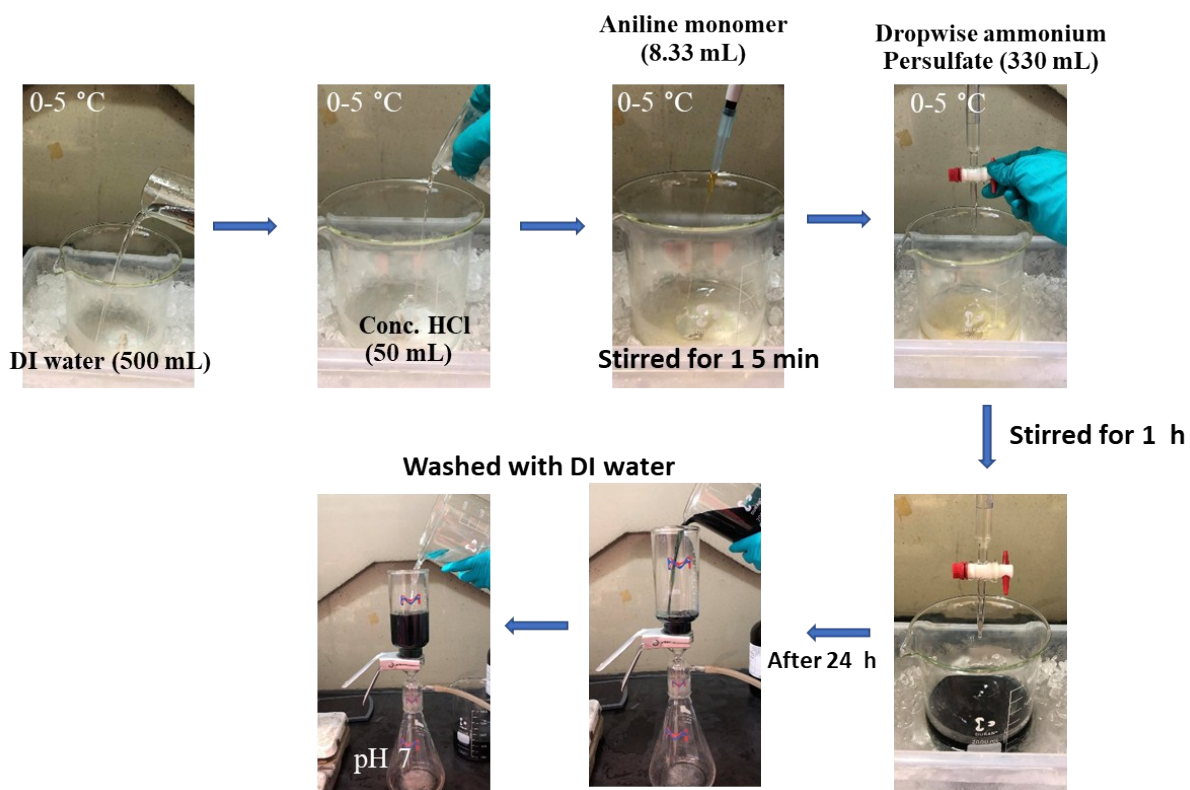


Fig. S2 Synthesis process of PANI.

In order to graft PANI on HyPE, the as-modified HyPE was immersed in PANI suspension in water for 1 h at room temperature. Then, the excess PANI solution and by-

product were removed using DI water and the grafted PANI on HyPE separator was dried overnight at 60°C. The amine group in the backbone of PANI structure is chemically bonded with the carboxyl group on the HyPE via the amide coupling reaction. Note, a mass loading of PANI is ca. 0.92 mg cm<sup>-2</sup>.

#### *Preparation of sulphur-carbon core-shell material*

Briefly, sulphur and carbon black were mixed together with a weight ratio of 2:1, respectively via ball milling machine for 2 h. Then, blended materials were further mixed by a mechano-fusion process (NOBILTA, model NOM-130, Japan) for 12 min at a rotation speed of 5000 rpm with a water-cooling system at 40 °C. Sulphur-carbon core-shell material was collected and used without further purification<sup>2</sup>.

#### *Structural and chemical characterizations*

The field-emission scanning electron microscopy (FE-SEM, JSM-7610F, JEOL) was used to characterize the morphologies of the as-modified materials. The energy dispersive X-ray spectrometry (EDX) equipped with FE-SEM machine provides the element mapping of the materials. The chemical surface analysis was evaluated by Fourier transform infrared spectroscopy (FTIR, PerkinElmer) and X-ray photoelectron spectroscopy (XPS, JPS-9010MC, JEOL) with Mg-K $\alpha$  radiation source ( $h\nu = 1253.6$  eV). The electrolyte wettability was analysed by measuring the contact angle using a contact angle goniometer (L2004A1-UK, Ossila). The 5  $\mu$ L of electrolyte was dropped on separator. The *in situ* UV adsorption was performed using AUTOLAB potentiostat (Metrohm, PGSTAT 302N) equipped with spectrometer (ULS2048L, AvaSpec) running NOVA software (version 1.11).

#### *Fabrication of Li-S batteries and electrochemical evaluations*

90 wt.% of as-prepared sulphur-carbon core-shell material was mixed with 10 wt.% PVDF and dissolved in NMP solution. After kept the mixture stirring overnight, the slurry was casted on carbon fibre paper substrate by a casting machine (GELON) and then dried using the vacuum oven at 60°C overnight. Note, a mass loading of sulphur active material is  $2.8 \pm 0.5$  mg cm<sup>-2</sup>. The casted paper was cut into a circle piece with a diameter of 1.58 cm using as a working electrode. The modification of HyPE with PANI with diameter 1.9 cm was inserted between the cathode and PE separator. Li chip was used as both reference and counter electrode. The electrolyte is the mixture of 1.0 M LiTFSI and 0.1 M LiNO<sub>3</sub> additive in 1:1 (by volume) of DOL and DME solution. Note, the amount of electrolyte usage is 15  $\mu$ L per mg of sulphur active material. The LSBs were assembled with coin-cell type batteries model CR2032 in an argon-filled glovebox (H<sub>2</sub>O and O<sub>2</sub> level less than 0.1 ppm, MBraun,

Germany). The cycling voltammetry (CV) was performed using the AUTOLAB potentiostat (Metrohm, PGSTAT 302N) running NOVA software (version 1.11) with a potential range of 1.6-3.0 V vs. Li/Li<sup>+</sup> using a scan rate of 0.2 mV s<sup>-1</sup>. The rate capability and stability performance were carried out using galvanostatic charge-discharge (GCD) technique via battery testers (GELON) in a potential range of 1.6-3.0 V vs. Li/Li<sup>+</sup> at 0.1-1.0C (1C = 1675 mA g<sup>-1</sup>). The electrochemical impedance spectroscopy (EIS) was performed using the AUTOLAB potentiostat (Metrohm, PGSTAT 302N) running NOVA software (version 1.11). The frequency is a range from 0.01 Hz to 100 kHz with a perturbation amplitude of 5 mV. Note that the as-fabricated cells were typically aged for 24 h before evaluating the electrochemical testing.

### *Investigation of polysulfide adsorption*

In order to evaluate the adsorption capability of the as-modified HyPE/PANI, the conventional H-type glass cell was demonstrated. Lithium polysulfide solution (1 M L<sup>-1</sup> of Li<sub>2</sub>S<sub>6</sub> in DOL/DME 1:1 by volume) was contained on the left chamber (dark colour) while blank solvent of DOL/DME (1:1 v/v) was placed in the right. PE as well as the incorporation of modified separator were inserted in the middle of H-type glass. The experiment was carried on for 6 h with data collecting since the beginning (0 min), 10, 30, 60, 180, 360 min.

### *Ionic conductivity and electrolyte uptake (EU)*

The ionic conductivity was calculated by following equation;

$$\sigma = L/(R_e A)$$

where L is the separator thickness, R<sub>e</sub> is the high-frequency intercept of the semicircle with the real axis was ohmic resistant between the electrolyte and surface of the electrode obtained from Nyquist plots, and A is the contact area between the separator and the electrode<sup>3</sup>.

The electrolyte uptake (EU) was calculated by soaking weighed separator in electrolyte (1.0M LiTFSI and 0.1M LiNO<sub>3</sub> additive in 1:1 (by volume) of DOL and DME solution) at room temperature for 1 hr in an argon-filled glovebox (H<sub>2</sub>O and O<sub>2</sub> level less than 0.1 ppm, MBraun, Germany). The EU determined by following equation at different rest time before weighting;

$$EU = [(W - W_o)/W_o] \times 100\%$$

where W<sub>o</sub> and W are the separator weight before and after electrolyte absorption, respectively.

### *Diffusion coefficient*

The lithium-ion diffusion coefficient ( $D_{Li^+}$ ) can be calculated from the impedance plot of the low-frequency Warburg region by following the equation below;

$$D_{Li^+} = R^2 T^2 / 2 A^2 n^4 F^4 c^2 \sigma^2$$

where

R is gas constant (8.314 J/mol K)

T is absolute temperature (298 K)

A is surface area of working electrode (1.98 cm<sup>2</sup>)

n is number of electrons transferred in reaction (2)

F is Faraday's constant (96500 C/mol)

c is concentration of lithium present in the active material (0.0218 mol/cm<sup>2</sup>)

$\sigma$  is Warburg coefficient calculated from slope of  $Z_{re}$ - $\sigma$  plot

The lithium-ion diffusion coefficient ( $D_{Li^+}$ ) can also be calculated by cyclic voltammetry from the slope of the peak current ( $I_p$ ) and square root of the scan rate ( $V^{0.5}$ ) by following the Randle-Sevcik equation;

$$I_p = 2.69 \times 10^5 n^{3/2} A D_{Li^+}^{1/2} C_{Li^+} v^{1/2}$$

where

$I_p$  is the peak current

n is the number of electrons transferred in reaction (2)

A is the surface area of working electrode (1.98 cm<sup>2</sup>)

$D_{Li^+}$  is the lithium-ion diffusion coefficient

C is the change in the concentration of lithium ion (1.46 mol/cm<sup>3</sup>)

v is the scan rate

### Computational details

The hypothesis of the theoretical DFT calculations in this work bases on the correlation between the LPSs adsorption energy and lithium bond effect.<sup>4, 5</sup> The first approach is to confirm that the LPS molecules can adsorb on the PANI functional groups. The favourable adsorption is resulted in the negative binding energy between PANI functional groups and LPS molecules. All the calculations reported in this article were performed by the Gaussian16 computational package based on density functional theory (DFT). Full optimizations and property calculations for the total energies were accounted by the hybrid meta generalized gradient approximation (meta-GGA)<sup>6</sup> with M06-2X<sup>7</sup> Minnesota class exchange-correlation functional and the polarized double  $\zeta$  basis set 6-31G(d,p) were set for all atoms. The basis set superposition error (BSSE) of the intermolecular interaction was applied to the energy correction of the binding complexes. The convergence thresholds for self-consistency-field was set at  $10^{-6}$  Hartree. The calculated relative binding ( $E_b$ ) energies were defined as follow:

$$E_b = E_{\text{PANI/LPSs}} - E_{\text{LPSs}} - E_{\text{PANI}}$$

where  $E_{\text{PANI/LPSs}}$ ,  $E_{\text{LPSs}}$ , and  $E_{\text{PANI}}$  are the total energies of the LPSs adsorbed on the PANI (herein aniline trimer), the isolated LPSs molecule, and the isolated PANI, respectively.

### Supporting Figures and Tables

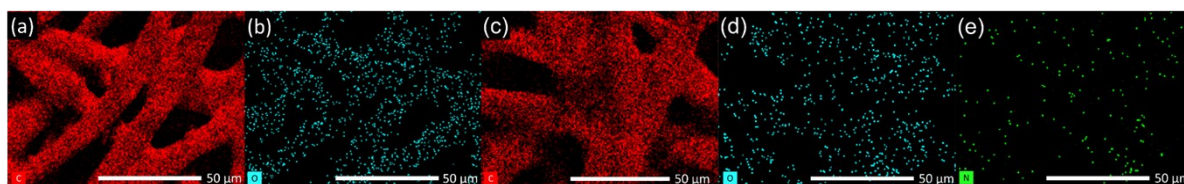


**Fig. S3.** EDX mapping of (a-b) HyPE, (c-e) HyPE-PANI-15.

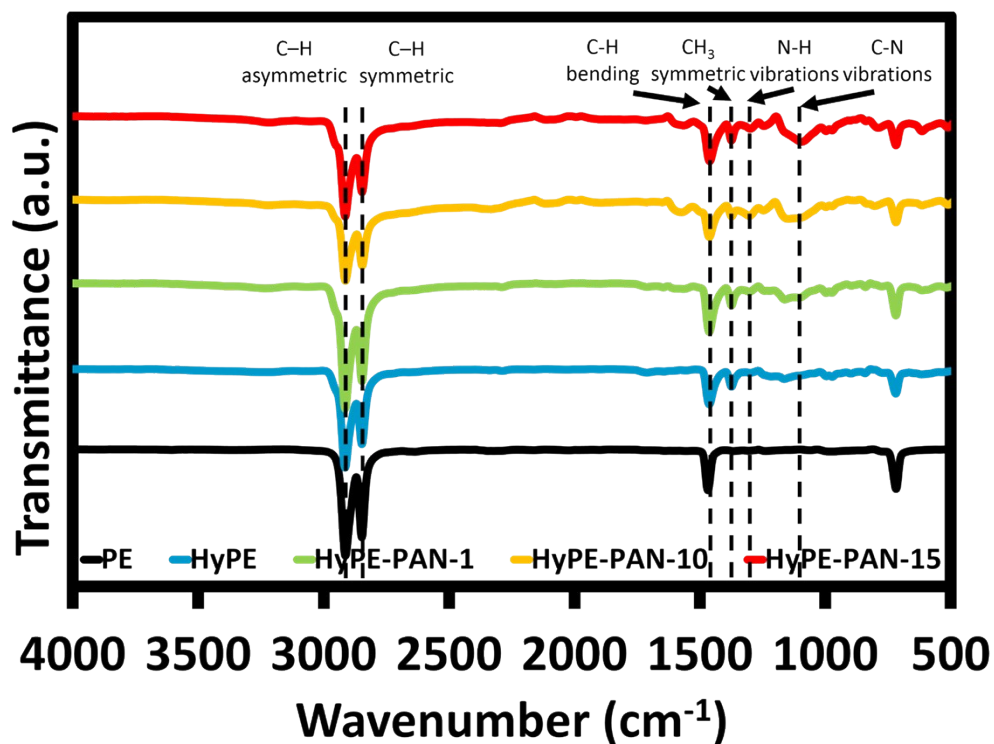


**Fig. S4.** FTIR spectra of PE, pristine HyPE, HyPE-PANI-1, HyPE-PANI-10, and HyPE-PANI-15.

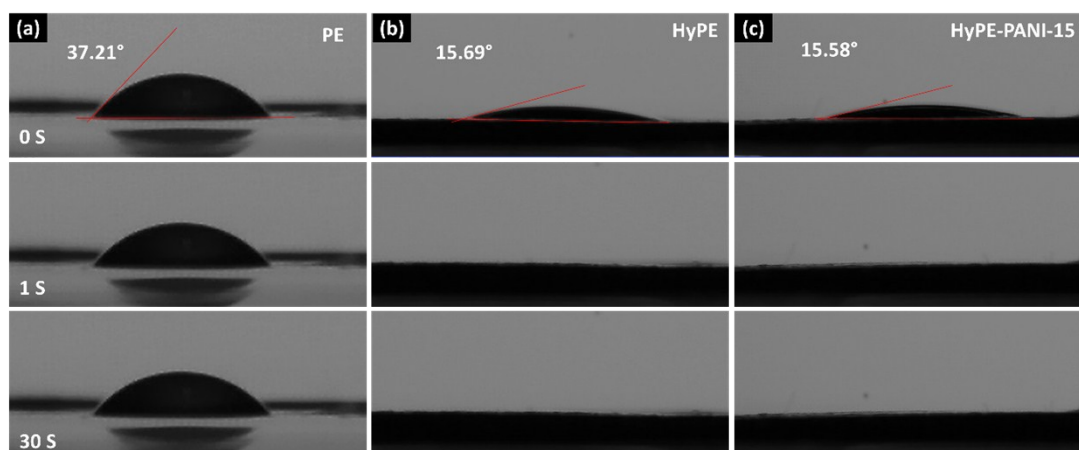


**Fig. S5.** The electrolyte wettability of different separators by using the contact angle test (a) PE (b) HyPE and (c) HyPE-PANI-15 in 1.0 M LiTFSI and 0.1 M LiNO<sub>3</sub> additive in DOL/DME.



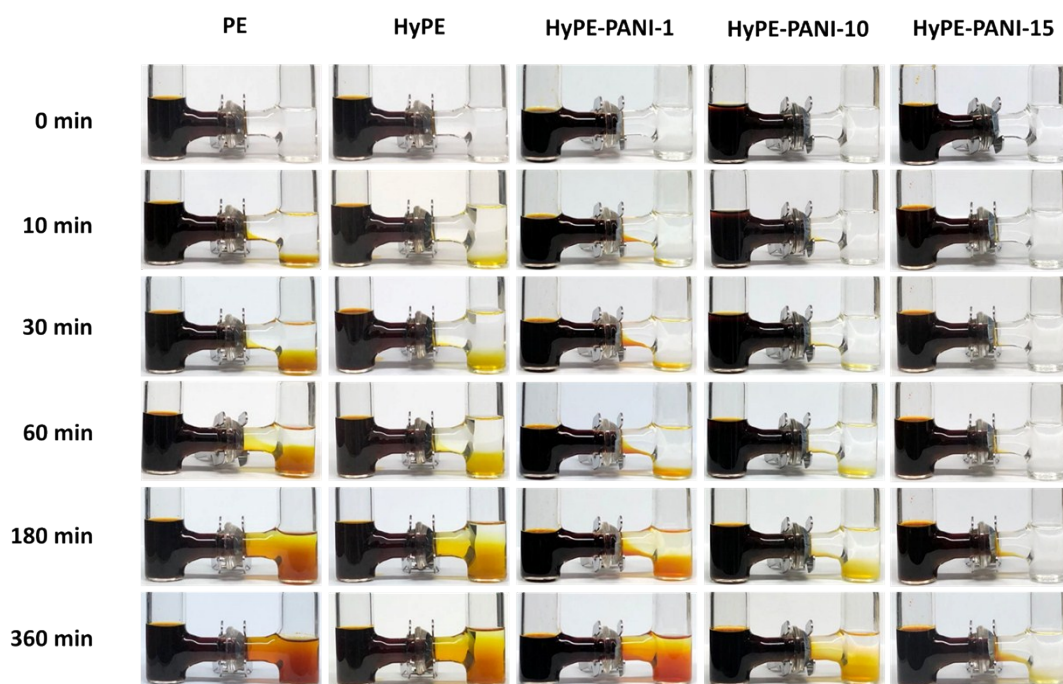


**Fig. S6.** The digital photographs of H-type glass cells contained with PE, HyPE, HyPE-PANI-1, HyPE-PANI-10, and HyPE-PANI-15 as the separators with different demonstrated times.

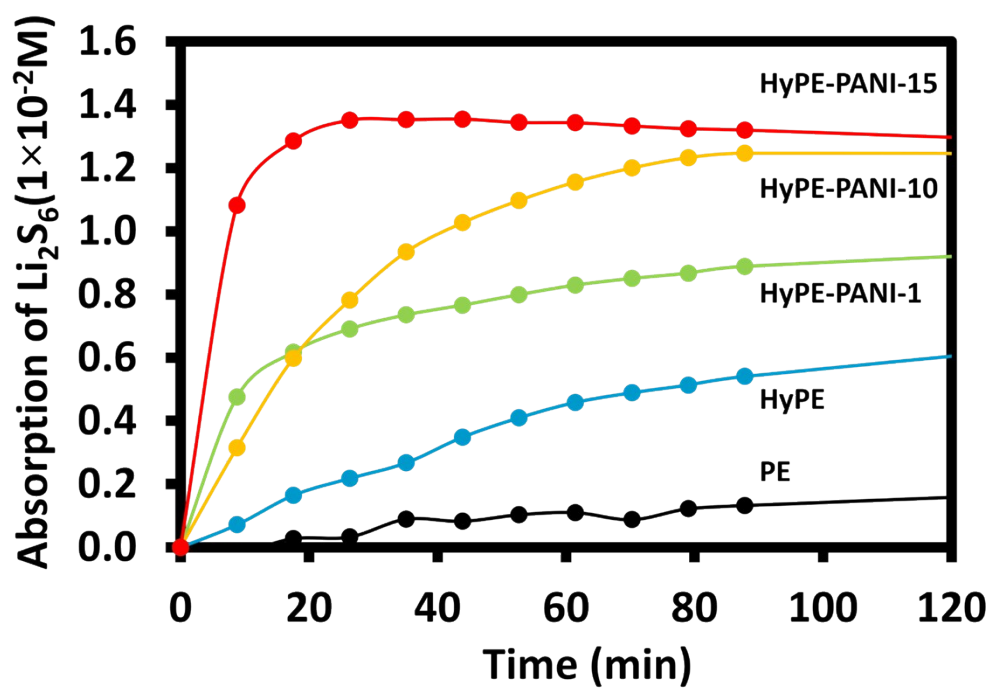


**Fig. S7.** Absorption capability of LPs of PE, HyPE, HyPE/PANI-1, HyPE/PANI-10, and HyPE/PANI-15 with varying times.

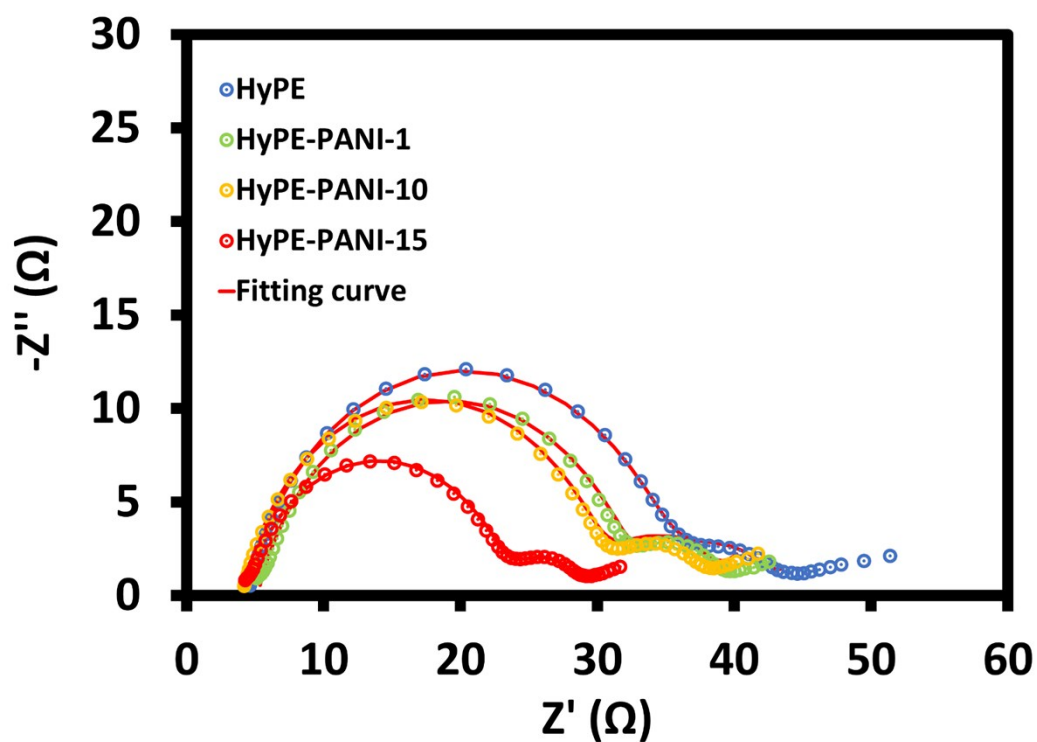


Table S1. The electrolyte uptake (EU) of different separators at different rest time before weighting after immersed in the electrolyte for 1 hr.

Sample	Rest Time (min)	EU (%)
PE	1	161.90
	5	123.81
	10	107.14
HyPE	1	172.73
	5	144.32
	10	127.27
HyPE-PANI-15	1	185.56
	5	157.78
	10	132.22

Table S2. The ionic conductivity of LSBs using different separators.

Sample	Ionic conductivity ( $\text{mS cm}^{-1}$ )
PE	7.29
HyPE	18.63
HyPE-PANI-15	19.22



**Fig. S8.** Nyquist plots of LSBs with varying separators.

**Table. S3.** Fitted values of LSB cells using HyPE and PANI-modified PANI separators.

Sample	$R_e$ ( $\Omega$ )	CPE'		$R_g$ ( $\Omega$ )	CPE		$R_{ct}$ ( $\Omega$ )	$W_0$
		$Y_1$ ( $m\Omega^{-1}$ )	$n_1$		$Y_2$ ( $\mu\Omega^{-1}$ )	$n_2$		$Y_3$ ( $\Omega^{-1}$ )
HyPE	4.41	13.4	0.670	7.50	27.0	0.830	30.9	0.90
HyPE-PANI-1	5.18	6.0	0.910	5.80	30.5	0.819	27.6	0.65
HyPE-PANI-10	4.12	9.0	0.736	8.06	21.8	0.846	26.4	0.49
HyPE-PANI-15	4.30	13.4	0.741	5.12	33.7	0.813	19.2	0.97

Note. Different concentrations of polyaniline precursors (0.10, 1.03 and 1.54 M) were deposited on HyPE separators marked as HyPE-PANI-1, HyPE-PANI-10, and HyPE-PANI-15, respectively

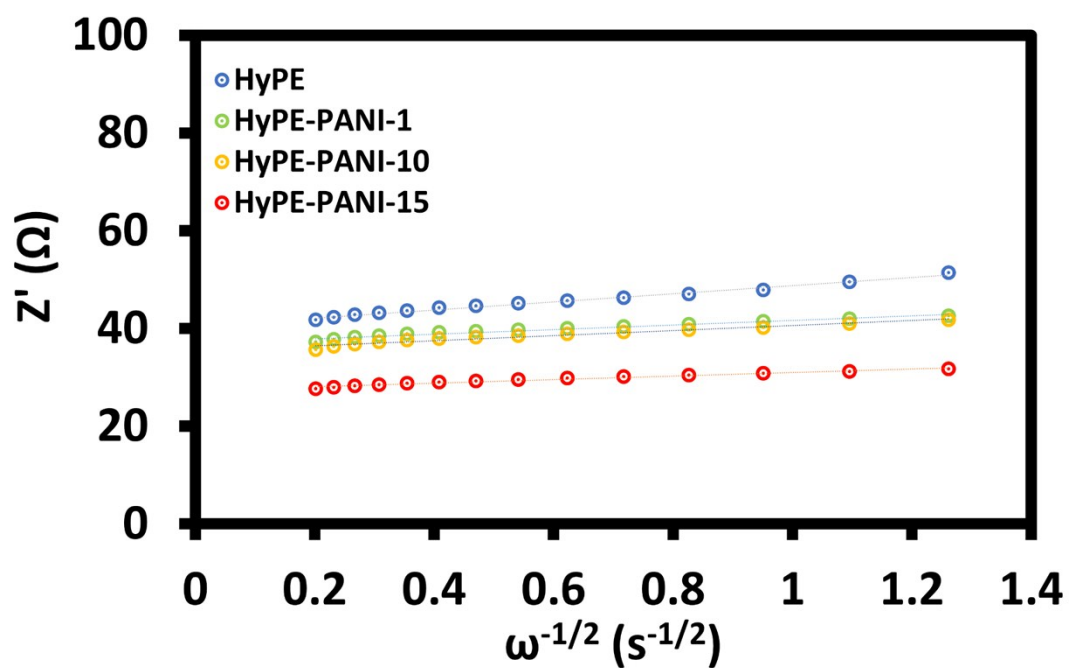


Fig. S9 The impedance plot of the low-frequency Warburg region of all LSBs using different separators.

**Table S4.** The diffusion coefficients of lithium ions ( $D_{Li^+}$ ,  $cm^2 s^{-1}$ ) in LSBs using different separators determined by EIS.

Sample	$D_{Li^+}$ ( $cm^2 s^{-1}$ )
PE	$4.48 \times 10^{-13}$
HyPE	$1.77 \times 10^{-14}$
HyPE-PANI-1	$5.61 \times 10^{-14}$
HyPE-PANI-10	$4.60 \times 10^{-14}$
HyPE-PANI-15	$9.15 \times 10^{-14}$

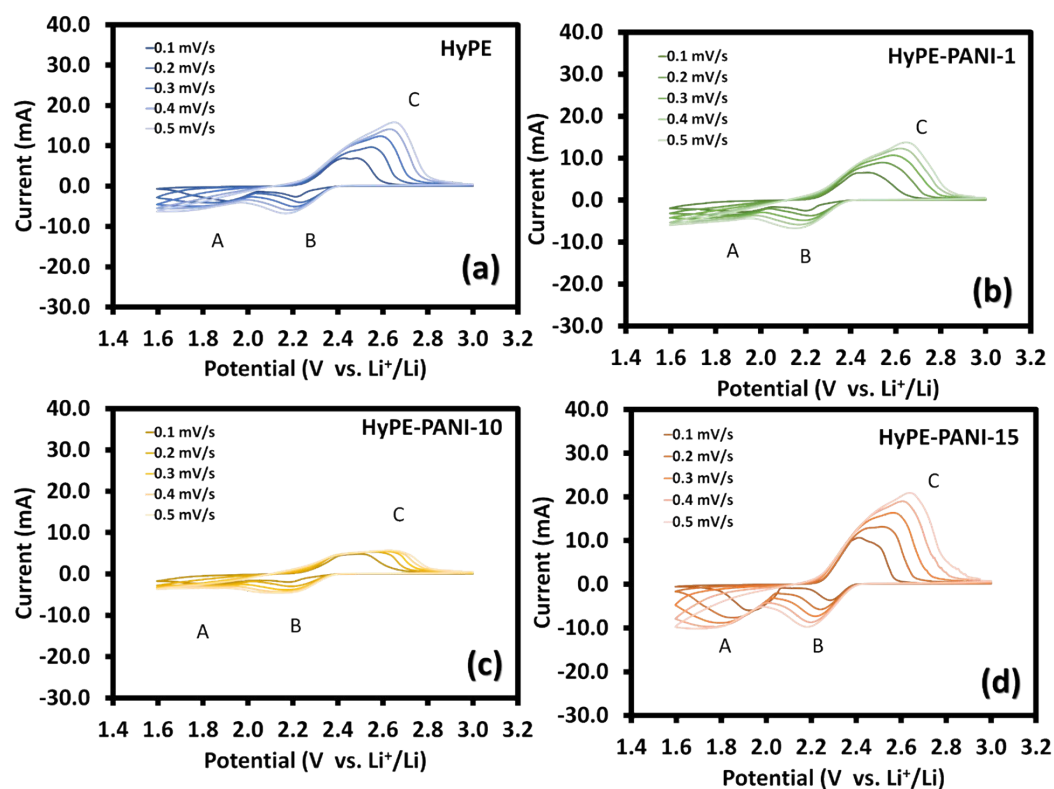


Fig. S10 Cyclic voltammograms of LSBs using different separators.

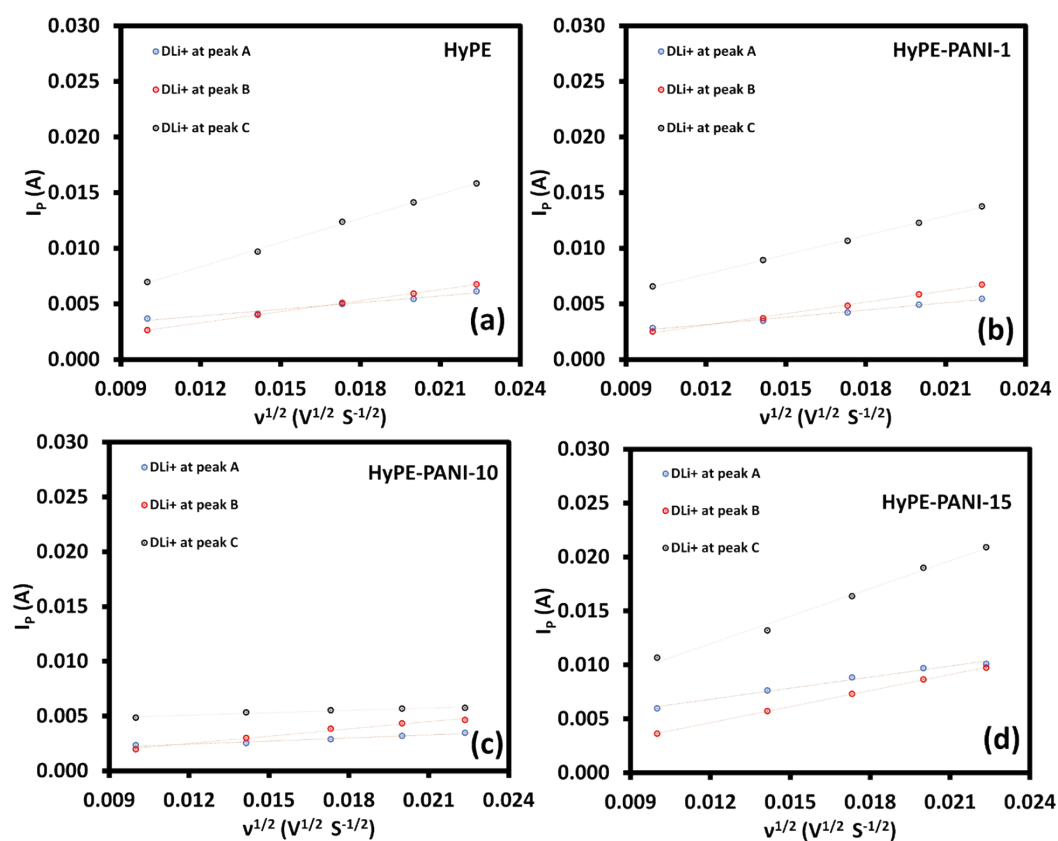


Fig. S11 The peak current vs. and square root of the scan rate ( $V^{0.5}$ ) plots.

**Table S5.** The diffusion coefficients of lithium ions ( $D_{Li^+}$ ,  $\text{cm}^2 \text{s}^{-1}$ ) in LSBs using different separators determined by CV.

Diffusion coefficient	PE	HyPE	HyPE-PANI-1	HyPE-PANI-10	HyPE-PANI-15
$D_{Li^+}$ at peak A	$2.71 \times 10^{-15}$	$8.51 \times 10^{-15}$	$9.9703 \times 10^{-15}$	$1.85 \times 10^{-15}$	$2.47 \times 10^{-14}$
$D_{Li^+}$ at peak B	$3.65 \times 10^{-14}$	$2.32 \times 10^{-14}$	$2.4992 \times 10^{-14}$	$1.04 \times 10^{-14}$	$5.19 \times 10^{-14}$
$D_{Li^+}$ at peak C	$2.66 \times 10^{-13}$	$1.11 \times 10^{-13}$	$7.0794 \times 10^{-14}$	$1.07 \times 10^{-15}$	$1.53 \times 10^{-13}$

## References

1. J. C. Eriksson, C. G. Götzlander, A. Baszkin and L. Ter-minassian-saraga, *Journal of Colloid and Interface Science*, 1984, **100**, 381-392.
2. P. Chiochan, N. Phattharasupakun, J. Wutthiprom, M. Suksomboon, S. Kaewruang, P. Suktha and M. Sawangphruk, *Electrochimica Acta*, 2017, **237**, 78-86.
3. J. Zhang, L. Yue, Q. Kong, Z. Liu, X. Zhou, C. Zhang, Q. Xu, B. Zhang, G. Ding, B. Qin, Y. Duan, Q. Wang, J. Yao, G. Cui and L. Chen, *Scientific Reports*, 2014, **4**, 3935.
4. T.-Z. Hou, W.-T. Xu, X. Chen, H.-J. Peng, J.-Q. Huang and Q. Zhang, *Angewandte Chemie International Edition*, 2017, **56**, 8178-8182.
5. T. Maihom, S. Kaewruang, N. Phattharasupakun, P. Chiochan, J. Limtrakul and M. Sawangphruk, *J. Phys. Chem. C*, 2018, **122**, 7033-7040.
6. Y. Zhao and D. G. Truhlar, *The Journal of Physical Chemistry A*, 2004, **108**, 6908-6918.
7. S. F. Boys and F. Bernardi, *Molecular Physics*, 1970, **19**, 553-566.